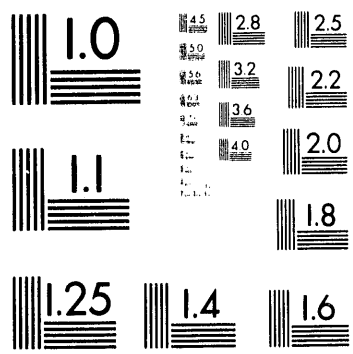
1.0
1.1
1.25
1.4
1.6
1.8
2.0
2.2
2.5
2.8
3.2
3.6
4.0
4.5
5.0

1 of 1

Conf-9308122--13

UCRL-JC-114187
PREPRINT

High Strain Rate Superplasticity in Metals and Composites

T.G. Nieh
J. Wadsworth
K. Higashi

This paper was prepared for submittal to the
International Conference on Advanced Materials '93
Tokyo, Japan
August 31 - September 8, 1993

July 1993

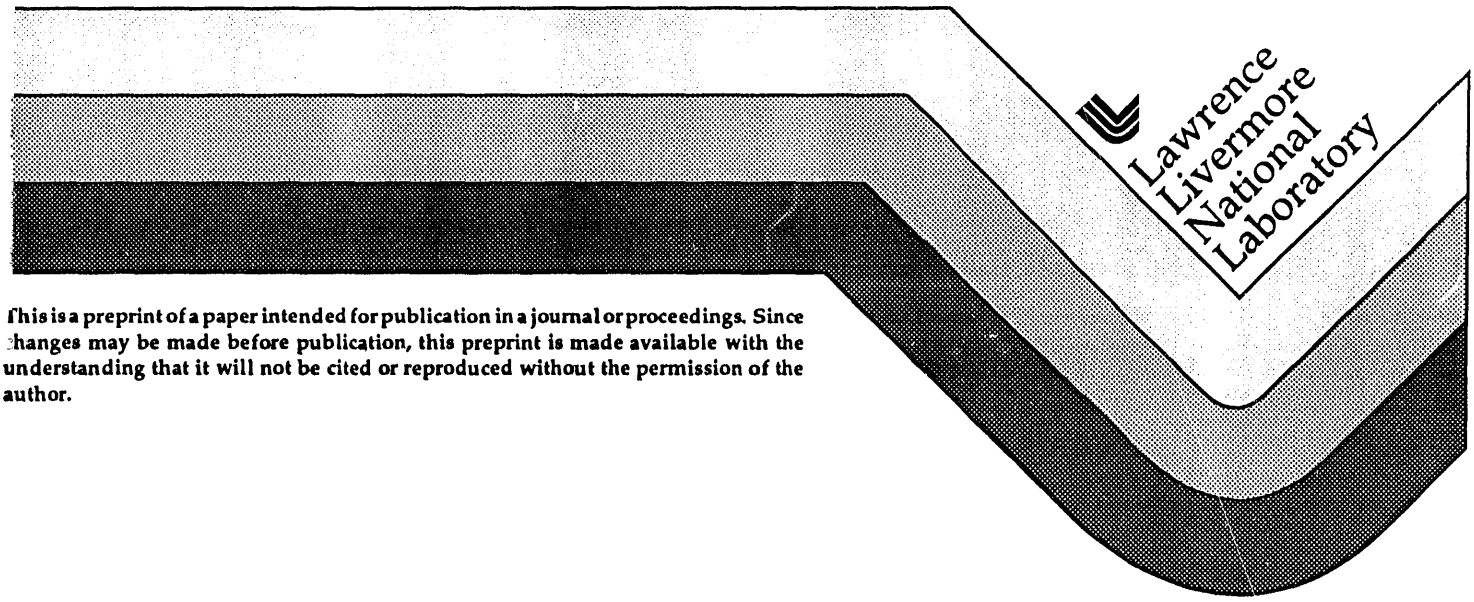

High Strain Rate Superplasticity in Metals and Composites

T.G. Nieh[a], J. Wadsworth[a], and K. Higashi[b]

[a] Lawrence Livermore National Laboratory, L-350, P.O. Box 808, Livermore, CA 94551, USA

[b] College of Engineering, Department of Mechanical Systems Engineering, University of Osaka Prefecture, Gakuen-cho, Sakai, Osaka 593, Japan

Superplastic behavior at very high strain rates (at or above 1 s^{-1}) in metallic-based materials is an area of increasing interest. The phenomenon has been observed quite extensively in metal alloys, metal-matrix composites (MMC), and mechanically-alloyed (MA) materials. In the present paper, experimental results on high strain rate behavior in 2124 Al-based materials, including Zr-modified 2124, SiC-reinforced 2124, MA 2124, and MA 2124 MMC, are presented. Except for the requirement of a fine grain size, the details of the structural requirements of this phenomenon are not yet understood. Despite this, a systematic approach to produce high strain rate superplasticity (HSRS) in metallic materials is given in this paper. Evidences indicate that the presence of a liquid phase, or a low melting point region, at boundary interfaces is responsible for HSRS.

1. BACKGROUND AND DISCUSSION

One of the major drawbacks of conventional superplastic forming is that the superplasticity is only found at relatively low strain rates, approximately 10^{-4}–10^{-3} s^{-1}. Recently, studies have demonstrated that superplasticity can exist at considerably higher strain rates than 10^{-3} s^{-1}.

So far, this high strain rate superplasticity (HSRS) phenomenon has been observed in metal-matrix composites [1-6], mechanically-alloyed alloys [7-11], and in some conventionally-produced metallic alloys [12-14]. A summary of published HSRS results is given in Table 1.

Table 1 HSRS Aluminum Alloys and Composites*

Material/Reference	Test Temp, °C	Solidus, °C	Strain Rate, (s^{-1})	Stress, (MPa)	Elong., %
Composites					
β SiC_w/2124 Al [1]	525	502	0.3	~10	~ 300
β $Si_3N_{4(w)}$/2124 Al [2]	525	502	0.2	~10	~ 250
α $Si_3N_{4(w)}$/7064 Al [3]	525	~ 525	0.2	~15	~ 250
β $Si_3N_{4(w)}$/6061 Al [4]	545	582	0.5	~20	~ 450
27wt%β SiC_w/7075 Al+ [5]	~500	< 538	0.2	40	--
AlN/6061 Al [6]	600	582	0.5	10	350
TiC/2014 Al [6]	545	507	0.2	15	250
Mechanically-alloyed Al					
IN 9021 [7]	475	495	1	30	~ 300
IN 9021 [8]	550	495	50		~ 1250
IN 90211 [9]	475	495	2	30	~ 500
MA $SiC_{(p)}$/IN9021 [10]	550	495	10	~7	~ 500
IN9052 [11]	590	--	10	18	330
Alloys					
7475 Al-0.9wt% Zr [12]	520	< 538	0.3	13	~ 900
7475 Al-0.7wt% Zr [12]	520	< 538	0.05	5	~ 900
2124 Al-0.6wt% Zr [13,14]	475	502	0.3	34.5	490

* Subscripts (w) and (p) denote whisker and particulate, respectively.
+ Compression

Grain boundary sliding is generally believed to be the dominant deformation mode in fine-grained, superplastic alloys. In the case of grain boundary sliding, grain size is certainly the most dominant microstructural parameter. This is reflected in the constitutive or phenomenological equations for superplastic flow and slip creep, generally expressed as [15],

$$\dot{\varepsilon} = A \cdot d^{-p} \cdot D \cdot \left(\frac{\sigma}{E}\right)^{n} \qquad (1)$$

where $\dot{\varepsilon}$ is the strain rate, D is the diffusivity, d is the grain size, σ is the stress, E is the modulus, n is the stress exponent, p is the grain size dependence, which is typically 2-3, and A is a material constant. According to eq. (1), refinement of the grain size by a factor of 2 would be expected to increase the optimum strain rate for superplastic flow by a factor of from 4 to 8 depending upon the precise grain size relationship as described above.

An overview of the superplastic behavior of metal alloys, and in particular Al alloys, to demonstrate the effect of grain size is given in Fig. 1. In this figure, the elongation-to-failure is shown as a function of strain rate for (i) 7475 Al, (ii) a USSR alloy V96Ts [16] that is rather similar in composition to the 7000 series alloy (but contains Zr as a grain refining element instead of Cr), (iii) Al-Li 2090 alloy, (iv) the commercial SUPRAL alloys, (v) SiC_w/Al and $Si_3N_{4(w)}$/Al composites, (vi) a Zr-modified Al 2124, and (vii) mechanically-alloyed IN9021 (AL 9021). The grain size ranges of these alloy groups are 10-20 μm for the 7475 Al alloys, about 5 μm for the USSR alloy, 2-3 μm for the 2090 Al and SUPRAL alloys, 1 μm or less for the SiC_w/Al composites and Zr-modified Al 2124, and 0.5 μm for IN9021. The general prediction of eq.(1), namely, that there is an increased strain rate for optimal superplastic flow with a decrease in grain size, is clearly illustrated in Fig. 1.

The generation of a new set of microstructural conditions to make grain-boundary sliding more facile, and to inhibit the intervention of power-law slip creep processes, can increase the maximum strain rate for superplastic flow. The most straightforward structural feature that can be modified to achieve such an enhancement in superplasticity is obviously a decrease in the grain size. The fields of materials and materials processing have been greatly improved in recent years; our knowledge of materials processing has advanced to the stage that the microstructure of a material can be tailored and controlled. In the following sections, we will present experimental results from the 2124 Al-based materials. A systematic approach will be given to illlustrate that superplasticity can be enhanced through grain size refinement.

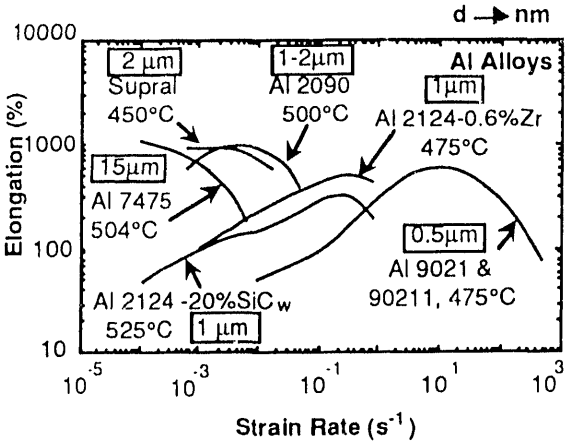

Fig. 1 An overview of superplastic behavior in metal alloys, illustrating the grain size effect.

1.1 Conventional I/M 2024 Al and P/M 2124 Al

Coarse-grained (≈ 50 μm) ingot-metallurgy (I/M) 2024 Al and powder-metallurgy (P/M) 2124 Al (≈ 20 μm) samples were prepared and tested. The high-temperature deformation properties of these coarse-grained alloys, depicted in Fig. 2, are noted to be quite similar. The stress exponent values for both alloys are approximately 5. Both alloys (I/M and P/M 2124 Al) exhibit power-law breakdown behavior at a strain rate of about 10^{-1} s^{-1}, similar to the case of pure aluminum [17]. Neither 2024 nor 2124 Al alloys are superplastic.

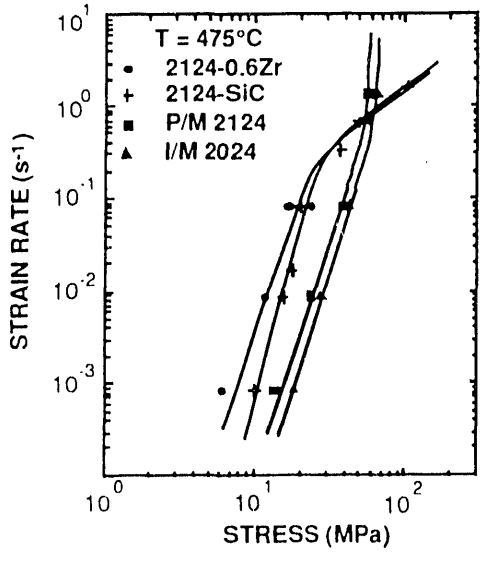

Fig. 2 Deformation properties of 2124 Al-0.6%Zr, SiC_w-2124 Al, I/M 2024 Al and P/M 2124 Al.

1.2 Zr-modified 2124 Al

The grain structure of the above I/M and P/M 2124 Al can be greatly reduced through Zr addition. For example, the grain size of 2124 Al containing 0.6%Zr is about 1 μm. This alloy, after thermomechanically processing, can exhibit superplasticity. The elongations-to-failure, as a function of the initial strain rate, at temperatures of 425, 450, 475 and 500°C are shown in Fig. 3. At the low strain rates, values of elongation-to-failure for the processed material are not much better than that of the as-received material. The ductility is noted to increase with increase in the initial strain rate and reaches a maximum at a strain rate of about 10^{1}–10^{0} s^{-1} for all testing temperatures. Optimum ductilities of 400-500% were obtained at temperatures near 475°C, and at a strain rate of 3.3×10^{-1} s^{-1}. The strain rate is almost 10 to 100 times higher than the strain rates at which superplasticity occurs in most advanced aluminum alloys, such as 7475 Al and Al-Li alloys [18,19].

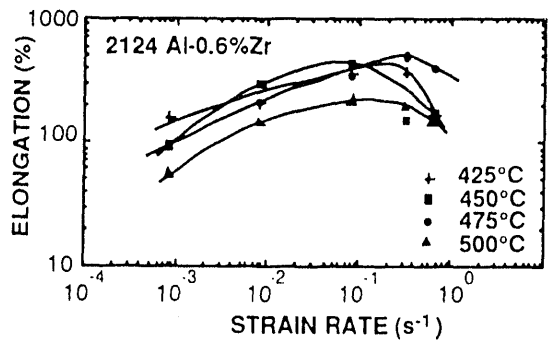

Fig. 3 Elongation-to-failure as a function of strain rate for 2124-0.6%Zr alloy at various temperatures.

The logarithm of strain rate as a function of the logarithm of flow stress for the 2124-0.6%Zr alloy is given in Fig. 2. The stress exponent, n, is noted to be about 5 in the low strain rate (or stress) regime. As strain rate increases, there is apparently a transition in the flow properties. In the high strain rate regime ($\geq 10^{-1}$ s^{-1}), the n values decrease to about 2. This decrease in the n value is consistent with the result that the tensile elongation of the alloy also increases with increasing strain rate. It also suggests that the ductility of the alloy at high temperatures is controlled by neck instability, in a manner similar to most other superplastic metal alloys [20].

From the above results, it is apparent that the addition of 0.6%Zr to 2124 Al, which results in a refinement of grain size, can produce HSRS in the alloy. To examine the effect of grain size on the deformation properties of this Zr-modified alloy, it is noted in Fig. 3 that, in the low strain rate regime, the strain rate for the fine-grained 2124-Zr is about 100 times faster than that for the coarse-grained (both I/M and P/M) materials. Nonetheless, the stress exponent values for all these alloys are approximately 5, In the high strain rate regime ($>10^{-1}$ s^{-1}), however, the curve for the 2124-Zr deviates greatly from those of 2124 and 2024 Al. While, both 2024 and 2124 alloys exhibit power-law breakdown behavior, a grain boundary sliding (GBS) mechanism apparently begins to intervene in the fine-grained 2124-Zr alloy. This prevalent GBS mechanism results in HSRS in the fine-grained 2124-Zr alloy.

1.3 Mechanically-alloyed 2124 Al (IN 9021)

One way to refine the grain size of an alloy is by mechanical alloying. The mechanically-alloyed version of 2124 Al is IN9021 (or Al 9021) which has a chemical composition (by wt%) of 4.0% Cu, 1.5% Mg, 1.1%C, 0.8%O, and balance Al. In addition to the S phase (CuMgAl) precipitates, normally present in 2124 Al, the MA alloy contains oxide and carbide dispersions of approximately 30 nm in diameter that have an interparticle spacing of about 60 nm. The grain size is about 0.5 μm.

The elongation-to-failure for IN9021 alloy, as a function of the initial strain rate, is shown in Fig. 4 for several temperatures. Over the temperature range from 425 to 500°C and at the strain rates at which most aerospace aluminum alloys exhibit superplasticity, i.e., 10^{-4}-10^{-3} s^{-1}, IN9021 shows a ductility typical of most pure metals and alloys, that is, 30-40%. However, the values of elongation-to-failure for IN9021 are observed to increase continuously as the strain rate increases. At extremely fast strain rates, nearly 1 s^{-1}, extended ductility was recorded. The maximum ductility, about 300%, was obtained at or above the high strain rate of 6.7×10 s^{-1}. At 500°C there appears to be a significant ductility loss by comparison with the lower temperature range. However, the trend of increased ductility as the strain rate is increased is still observed. At the highest strain rate (~ 1.3 s^{-1}), which corresponds to the highest value of elongation-to-failure (300%), a relatively high value of strain rate sensitivity (m = 0.3) was observed. The general characteristics of the curves in Fig. 4 are noted to be similar to those for the fine-grained, Zr-modified 2124 Al, shown in Fig. 3. The optimal superplastic strain rate for IN-9021 is also noted to be higher than that for the Zr-modified 2124 Al, resulting from a finer grain size. It is important to point out that Higashi *et al.* [7] have tested IN-9021 and obtained a maximum value of elongation of 1250% at 550°C and at a very high strain rate of 50 s^{-1}. This result is also included in Fig. 4.

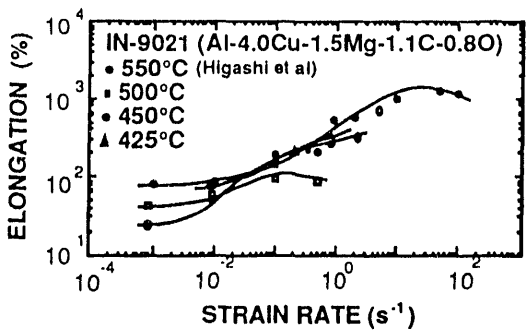

Fig. 4 Elongation to failure for IN9021 showing HSRS superplasticity.

1.4 2124 Al-based Metal-Matrix Compoistes

An additional method to produce HSRS through grain size refinement is by adding ceramic reinforcements, i.e., MMC. The microstructure of a MMC is, in general, very complex and the grain size is approximately 1 μm. Reinforced 2124 Al composites can be made by adding either SiC or Si_3N_4 whiskers to the matrix alloy. Many of these MMCs have been demonstrated to be superplastic at high strain rates. As shown in Table 1, the maximum elongation value of SiC_w/2124 Al is about 300% and is found at 525°C.and at a strain rate of 0.3 s^{-1}. Rather low strain rate sensitivities ($m \sim 0.1$), and thus low elongations to failure (<100%), were generally observed at low strain rate regions.

It is noted that 525°C is above the solidus temperature of the 2124 Al matrix (502°C). Mechanical tests were also carried out on the composite at temperatures of 475 and 500°C (i.e. below the solidus temperature), and at 550°C (i.e. yet further above the solidus temperature); these results are depicted in Fig. 5. The data in Fig. 5 show that, at high strain rates, the values of strain rate sensitivity increased to about 0.3 at all temperatures, and corresponding high values of elongation-to-failure were also recorded in these strain rate regimes. The data in Fig. 5 indicate that the flow characteristics do not exhibit a discontinuity across the solidus temperature, suggesting that the presence of partial liquid phase may be not a unique contributing factor to the observed superplasticity.

It should be pointed out that HSRS is not universally observed in fine-grained Al-based MMC composites. Table 2 lists the SiC_w- and $Si_3N_{4(w)}$-reinforced composite combinations that are superplastic and non-superplastic. As shown in Table 2, specific combinations of matrix and whiskers in a MMC are critical to the development of HSRS. A simple criterion for superplasticity based on the individual types of whisker or alloy matrix appears to be impossible. This viewpoint is supported by the observation that β $Si_3N_{4(w)}$/2124 and β Si_3N_4/6061 are superplastic, but α $Si_3N_{4(w)}$/2124 and β SiC/6061 are not. Thus, a fine matrix grain size is a necessary but insufficient condition for the HSRS phenomenon. A basic understanding of the origin of HSRS in MMC is still unclear. However, it is generally agreed that the deformation process in these HSRS-MMC is interfacial sliding. This statement is indirectly supported by the fact that the fracture surface of superplastically-deformed specimens often exhibit extensive metallic covered fiber pull out, suggesting substantial sliding during deformation.

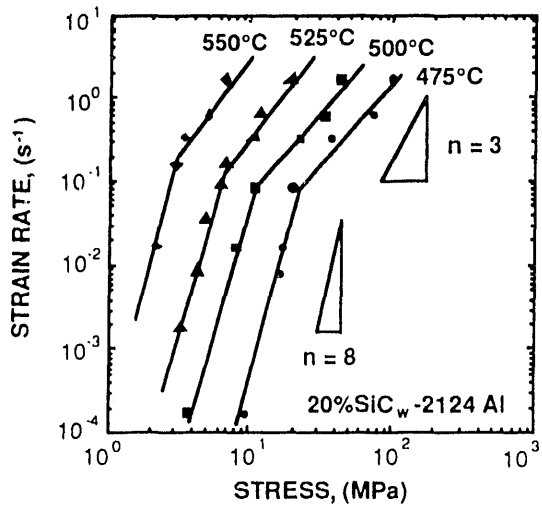

Fig. 5 Strain rate-stress data for Al 2124 containing 20 vol.% SiC whisker at various temperatures.

Table 2 Superplasticity in SiC_w and $Si_3N_{4(w)}$/Al

Matrix	Whisker	Superplastic?
2124 Al	β Si_3N_4	yes
6061 Al	β Si_3N_4	yes
7064 Al	α Si_3N_4	yes
2124 Al	α Si_3N_4	no
2124 Al	β SiC	yes
6061 Al	β SiC	no

1.5 Mechanically-alloyed MMC

Another method to produce a fine microstructure is by mechanical alloying of SiC particulate-reinforced 2124 Al [21]. This material, denoted as MA-SiC_p/IN9021, has a microstructure which

comprises the microstructure of IN9021 (grain size ~ 0.5 μm), superimposed with uniformly distributed SiC particulates (~5 μm in diameter).

Tensile true stress-true strain curves for the mechanically alloyed SiC_p/IN9021 aluminum composite are shown in Fig. 8 at strain rates from 10^{-3} to 100 s^{-1} and at a testing temperature of 550°C (823K). The curve for constant true strain rates over 5 s^{-1}, corresponding to the optimum superplastic strain rates, yielding an elongation value over 400%. Shown in Fig. 5 is the variation in elongation for the MA-SiC_p/IN9021 composite plotted as a function of strain rate for a testing temperature of 550°C (823K). Included in this figure are also results from the IN9021 alloy for comparison. The addition of SiC particles to IN9021 does not further refine the grain size of the material. As a result, the optimum superplastic strain rates for IN9021 and MA-SiC_p/IN9021 are virtually the same. However, the presence of additional SiC particles apparently causes a reduction of superplastic elongation; this is attributed to enhanced cavitation in the SiC-containing composite. The general behavior of the two materials, however, are similar.

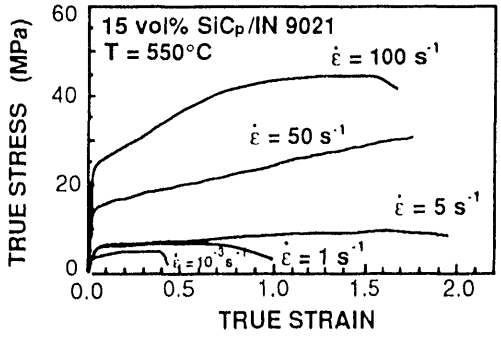

Fig. 6 True stress-true strain curves for the mechanically alloyed SiC_p/IN9021 composite.

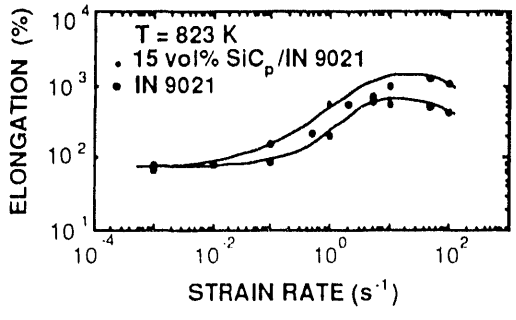

Fig. 7 Elongation vs strain rate for SiC_p/IN9021 composite and IN9021 alloy. (from Ref. 7)

2. ORIGIN OF HSRS

There is no doubt that grain size plays an important role in HSRS. Nonetheless, as shown in Table 2, the fact that HSRS was observed in some fine-grain materials, but not in other, presumably-similar, fine-grained materials demonstrates that there must exist other microstructural parameters contributing to HSRS.

It is pointed out in Table 1 that, despite some subtle differences in the experimental procedures and results, the tests were performed at temperatures near to or above the matrix solidus temperatures of the materials. In other words, materials were usually tested in a semi-solid state. (Some materials may have been tested at a nominal temperature which is slightly lower than the solidus. Because of the extremely fast strain rates, however, the effective temperature is expected to be significantly higher than the nominal test temperature, as a result of adiabatic heating.)

A question regarding the data in Fig. 5, and especially the data for 475°C, is that it is below the solidus of the 2124 Al matrix (505°C). The deformation properties of 475 and 525°C are, therefore, expected to be somewhat different. However, the data in Fig. 5 clearly indicate that the flow characteristics do not exhibit a discontinuity across the solidus temperature. The discrepancy is attributable to two possible factors – adiabatic heating during high rate deformation, and solute redistribution. In fact, the temperature rise during the high strain rate testing of SiC/2124 is estimated to be about 15°C (if no localized heating occurs). Therefore, although the apparent test temperature is 475°C, the actual temperature will be higher.

Another factor, which can also contribute to the presence of a liquid phase is related to solute segregation at a reinforcement-matrix interface. For example, Strangwood *et al.* [22] have used a special FEM/STEM technique to study solute segregation to SiC/Al alloys interfaces and showed that the Mg and Cu concentrations at the SiC/matrix interfaces in an underaged 15 vol%SiC_p-2xxx Al (1.45 at%Cu, 1.67 at%Mg, 0.12 at%Zr, 0.1 at%Mn) could reach about 4.5 and 9 at%, respectively. Both the Mg and Cu segregation are expected to reduce the local melting point of the Al matrix near the interface region. (The effects of Mg and Cu on the melting point of Al are estimated to be approximately -6°C/at%Mg and -6.5°C/at%Cu [23]).

Therefore, although the test temperature of 475°C in Fig. 5 (for SiC/2124 Al) appears to be within the solid range of 2124 Al, because of the Mg segregation, it may nonetheless be sufficiently high to result in local melting at the SiC/Al interface. For example, a Mg concentration of over 6.5 at% at the

interface can by itself result in localized melting at 475°C, even in the absence of adiabatic heating from high strain rate deformation. Therefore, the HSRS phenomenon may occur in the presence of some liquid, even though the temperature appears to be below the solidus in a SiC/Al or Si_3N_4/Al composite.

3. SUMMARY

High strain rate superplasticity (HSRS) has been observed in a number of materials, including modified conventional alloys, mechanically-alloyed alloys, and metal-matrix composites. Despite differences in the chemical compositions of the alloy matrix, all these materials show similar superplastic properties; namely, exhibiting a maximum elongation of over 300% at a strain rate of about 0.1–1 s^{-1}. The HSRS results are important since one limitation of current superplastic forming technology is the slow forming rate which is typically 10^{-5} to 10^{-3} s^{-1}. There exist some evidences suggesting that the presence of a liquid phase, resulting from the test conditions, or the presence of a low melting point region caused by solute segregation (e.g., at the whisker-matrix interface in metal-matrix composites, and at grain boudaries in alloys) may be responsible for the observed HSRS phenomenon. Upon high strain rate deformation, the above semi-solid materials behave like non-Newtonian fluids. A fine grain size is a necessary but insufficient condition for the observed HSRS phenomena.

4. ACKNOWLEDGEMENT

This work was performed under the auspices of the U.S. Department of Energy by LLNL under contract No. W-7405-Eng-48.

5. REFERENCE

1. T.G. Nieh, C.A. Henshall, and J. Wadsworth, *Scripta Metall.*, **18**, 1405 (1984).
2. T. Imai, M. Mabuchi, Y. Tozawa, and M. Yamada, *J. Mater. Sci. Lett.*, **9**, 255 (1990).
3. M. Mabuchi and T. Imai, *J. Mater. Sci. Lett.*, **9**, 763 (1990).
4. T. Imai, M. Mabuchi, and Y. Tozawa, in *International Conference on Superplasticity in Advanced Materials (ICSAM-91)*, eds. S. Hori, M. Tokizane, and N. Furushiro, The Japan Society for Research on Superplasticity, 1991, pp. 373-378..
5. A. Sakamoto, C. Fujiwara, and T. Tsuzuku, in *Proc. 13rd Jpn. Congress on Mater. Res.*, The Soc. of Mater. Sci., Japan, 1990, pp.73-79.
6. T. Imai, private communication, 1993.
7. T.G. Nieh, P.S. Gilman, and J. Wadsworth, *Scripta Metall.*, **19**, 1375 (1985).
8. K. Higashi, T. Okada, T. Mukai, and S. Tanimura, *Scripta Metall. Mater.* **25**, 2503 (1991).
9. T.R. Bieler, T.G. Nieh, J. Wadsworth, and A.K. Mukherjee, *Scripta Metall.*, **22**, 81 (1988).
10. K. Higashi, T. Okada, T. Mukai, and S. Tanimura, T.G. Nieh, and J. Wadsworth, *Scripta Metall. Maters.*, **26**, 185 (1992).
11. K. Higashi, T. Okada, T. Mukai, and S. Tanimura, *Mater. Sci. Eng.* A **159**, L1 (1992).
12. N. Furushiro, S. Hori, and Y. Miyake, in *International Conference on Superplasticity in Advanced Materials (ICSAM-91)*, eds. S. Hori, M. Tokizane, and N. Furushiro, The Japan Society for Research on Superplasticity, 1991, pp. 557-562.
13. T.G. Nieh and J. Wadsworth, in *Superplasticity in Aerospace-Aluminum*, edited by R. Pearce and L. Kelly, Ashford Press, Curdridge, Southampton, Hampshire, (1985), pp. 194-214.
14. T.G. Nieh and J. Wadsworth, *Scripta Metall. Mater.* **28**, 1119 (1993).
15. O.D. Sherby and J. Wadsworth, *Prog. Mater. Sci.*, **33**, 169, (1989).
16. M.X. Rabinovich, O.A. Kaibyshev, and V.G. Tufinov, *Metalloved Term Obrab Met.*, **3**, 55 (1978).
17. H. Luthy, A.K. Miller, and O.D. Sherby, *Acta Metall.*, **28**, 169 (1980).
18. M.W. Mahoney, A.K. Ghosh, and C.C. Bampton, in *ICCM 6 and ECCM 2*, edited by F.L. Matthew et al., Elsevier, 1987, pp. 2.372-2.376.
19. J. Wadsworth and A.R. Pelton, *Scripta Metall.*, **18**, 387 (1984).
20. D.A. Woodford, *Trans. ASM*, **62**, 291 (1969).
21. T.G. Nieh, C.M. McNally, J. Wadsworth, D.L. Yaney, and P.S. Gilman, in *Dispersion Strengthened Aluminum Alloys*, edited by Y-W Kim and W.M. Griffith, The Metallurgical Society, Warrendale, PA, 1988, pp. 681-692.
22. M. Strangwood, C.A. Hippsley, and J.J. Lewandowski, *Scripta Metall. Mater.*, **24**, 1483 (1990).
23. *Binary Alloy Phase Diagrams, Vol. 1*, edited by T. Massalski, J.L. Murray, L.H. Bennett, and H. Baker (ASM, Metals Park, Ohio, 1986).

DATE
FILMED
12/27/93
END